Effect of Suction on the Stability of Subsonic Flows over Smooth Backward-Facing Steps

Ayman A. Al-Maaitah,* Ali H. Nayfeh,† and Saad A. Ragab‡
Virginia Polytechnic Institute and State University, Blacksburg, Virginia 24061

The effect of suction on the stability of compressible flows over backward-facing steps is investigated. Mach numbers up to 0.8 are considered. As expected, suction considerably reduces the separation region. The results show that continuous suction stabilizes the flow outside the separation bubble as expected, but it destabilizes the flow inside it. Nevertheless, the overall N factor decreases as the suction level increases. This is due to the considerable reduction of the separation bubble. For the same suction flow rate, properly distributed suction strips stabilize the flow more than continuous suction. Furthermore, the size of the separation bubble, and hence its effect on the instability, can be considerably reduced by placing strips with high suction velocities in the separation region.

I. Introduction

THE increasing interest in high-performance aircraft has promoted more research in the area of laminar flow control (LFC). Boundary-layer transition does not only affect the lift and drag characteristics of lifting surfaces but it also affects airplane stability and control.[1] Surface imperfections have a significant effect on the transition process. Unfortunately, the sizes of some unavoidable imperfections cannot be always reduced to significantly diminish their effect. This demands the investigation of methods for controlling the flows around such imperfections. Such investigations must take into consideration the coexistence of different instability mechanisms in such flows.[2-5] In this work, we study the effectiveness of wall suction on the stabilization of flows around two-dimensional (2-D) backward-facing steps.

Carmichael et al.[6] and Carmichael and Pfenninger[7] performed flight experiments on the wing glove of an F-94A airplane. The modified 652-213 airfoil had 69 suction slots distributed between 41 and 95% chord. They investigated single and multiple sinusoidal waves located at 15, 28, and 64% chord. Their results show that the allowable sizes of the waves increase when embedded in the suction region. They found that to maintain laminar flow across the airfoil requires an 8% increase in the suction level over the clear airfoil case. Carmichael[8] established empirical criteria relating the height-to-width ratio of the waves to the Reynolds number. However, these criteria are valid only for the configurations and the conditions investigated in the experiments. Moreover, they do not indicate the minimum suction levels needed to reduce the effect of the waviness. Spence and Randall[9] investigated the effect of uniform suction on the stability of boundary layers over plates with sinusoidal surface waves. They derived a closed-form expression for the asymptotic mean profile. By using the parallel stability theory of Lin,[10] they calculated the suction velocity needed to make the critical Reynolds number larger than the flow Reynolds number. Separation was not taken into consideration. Their results show that as the wavelength increases smaller suction velocities are needed.

More recently, Nayfeh and Reed[11] and Reed and Nayfeh[12] proposed a numerical-perturbation scheme to study the effect of porous suction strips on the stability of boundary layers over axisymmetric bodies and flat plates. To optimize the effect of the porous strip configuration, they suggested the concentration of suction near branch I of the neutral stability curve. Their calculations show good agreement with the experiments of Reynolds and Saric[13] and Saric and Reed.[14] Hahn and Pfenninger[15] experimentally investigated the effect of suction on the transition over a backward-facing step. They placed closely spaced suction slots downstream of the step. Suction levels were found for the prevention of premature transition downstream. Their measurements show that suction considerably moves the reattachment region upstream. They found that suction is more effective when the strips are placed slightly upstream of the reattachment region. However, they stopped short of performing stability measurements.

Although existing investigations indicate that wall suction can be used to stabilize flows around surface imperfections, none gives a detailed physical explanation of how suction affects the stability. Questions about the most effective suction levels and distributions still need to be answered. Furthermore, an understanding of how the coexistence of different instability mechanisms alters the effectiveness of suction is still lacking.

To gauge the effectiveness of wall suction in controlling such flows, one needs to predict its effect on the transition location. A common method for predicting the transition location is the amplification or N factor of the instability waves. For two-dimensional boundary layers, the N factor is about 9.0, while for three-dimensional boundary layers on a swept wing the N factor is in the range of 7.0–11.0.[16,17] Moreover, Nayfeh et al.[5] studied the stability of flows around two-dimensional bulges. They correlated their results with the experiments of Walker and Greening (as reported in Fage[18]) and found that the N factor is in the range of 7.4–10.0. They also found that the most dangerous frequency is different from that for the flow over a flat plate. A similar behavior was confirmed by Cebeci and Egan.[19] Ragab et al.[20] extended the work of Nayfeh et al.[5] and investigated the stability of compressible flows over smooth two-dimensional backward-facing steps. Al-Maaitah et al.[21] investigated the effect of wall cooling on the stability of compressible flows over smooth

Received March 28, 1989; revision received Oct. 31, 1989.

*Assistant Professor, Department of Engineering Science and Mechanics. Muatah University, Jordan.

†University Distinguished Professor, Department of Engineering Science and Mechanics.

‡Associate Professor, Department of Engineering Science and Mechanics.

two-dimensional backward-facing steps. They found that there is an optimal cooling level beyond which more cooling results in destabilizing the flow.

In the present work, we investigate the effect of uniform suction as well as suction strips on the stability of flows over two-dimensional backward-facing steps. The mean profiles are calculated using the interacting boundary-layer equations[22] (IBL) modified for the case of wall suction. These equations account for the upstream influence resulting from the separation bubble and the suction strips. The stability of the mean profiles is calculated using a quasiparallel linear stability theory for two-dimensional compressible flows. The theory accounts for the coexistence of both viscous and shear-layer instabilities in the separation region. The effectiveness of suction is then measured by the reduction in the resulting N factor.

II. Mean Flow

We need to calculate the compressible subsonic flows around smooth 2-D backward-facing steps (see Fig. 1), considering the effect of uniform wall suction and concentrated suction strips. The steps under consideration produce small separation bubbles behind them. In such flows, there is a strong viscous-inviscid interaction and an upstream influence resulting from the separation bubble and the suction strips. The conventional boundary-layer formulation cannot predict such flows. For Mach numbers up to 0.8, we calculated the mean flows using the interacting boundary-layer equations. There is a very good agreement between the solutions of the Navier-Stokes equations[20,23] and the IBL equations. This is true for both the mean flow and the stability characteristics.

The flowfield is assumed to be governed by the nonsimilar boundary-layer equations. After applying the Prandtl transposition theorem and using the Levy-Lees variables, one can write these equations as

$$2\xi FF_\xi + VF_\eta - \frac{\partial}{\partial\eta}\left(\theta\frac{\partial F}{\partial\eta}\right) + \beta_0(F^2 - Q) = 0 \tag{1}$$

$$2\xi F_\xi + V_\eta + F = 0 \tag{2}$$

$$2\xi FQ_\xi + VQ_\eta - \frac{\partial}{\partial\eta}\left(\frac{\theta}{PR}\frac{\partial Q}{\partial\eta}\right) - (\gamma-1)M_\infty^2\frac{U_e^2}{T_e}\theta F_\eta^2 = 0 \tag{3}$$

where

$$F = \frac{u}{U_e}, \qquad Q = \frac{T}{T_e} \tag{4a}$$

$$V = \frac{\sqrt{2\xi}}{\rho_e U_e \mu_e}\left[\sqrt{Re}\,\rho w + \eta_x\sqrt{2\xi}\,F\right] \tag{4b}$$

$$\theta = \frac{\rho\mu}{\rho_e\mu_e} \quad \text{and} \quad \beta_0 = \frac{2\xi}{U_e}\frac{dU_e}{d\xi} \tag{4c}$$

The Levy-Lees coordinates ξ and η are given by

$$\xi(x) = \int_0^x \rho_e\mu_e U_e\,dx \quad \text{and} \quad \eta(x,z) = \frac{\sqrt{Re}\,U_e}{\sqrt{2\xi}}\int_0^z \rho\,dz \tag{5}$$

and the Prandtl transposed z and w variables are defined as

$$z = y - f[\zeta(x)], \qquad w = v - u\frac{df}{dx} \tag{6}$$

where $f(\zeta)$ is the shape of the wall defined as

$$f(\zeta) = \tfrac{1}{2}h[1 + \mathrm{erf}(\zeta)], \qquad \zeta = Re^{-3/8}\lambda^{5/4}(x-1) \tag{7}$$

In Eqs. (1–6), the velocities u and v are normalized with respect to the freestream velocity U_∞^*; lengths are normalized with respect to L^*, which is the distance from the leading edge to the center of the step; and the temperature, viscosity, and thermal-conductivity coefficients are normalized with respect to their freestream values T_∞^*, μ_∞^*, and κ_∞^*. Here

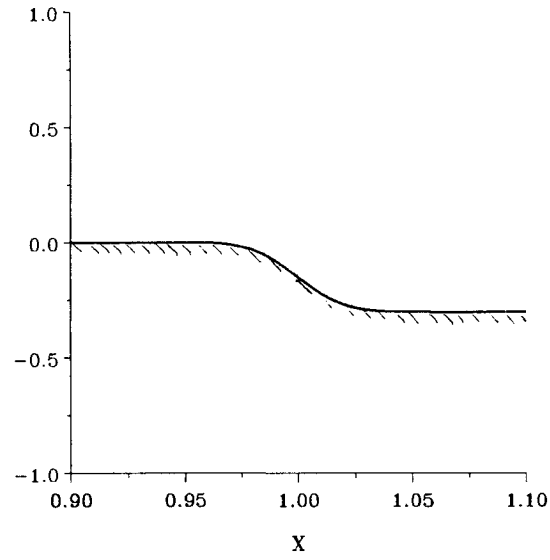

Fig. 1 A schematic of the backward-facing step. The normal coordinate is magnified ten times compared with the streamwise coordinate.

$$Re = \frac{U_\infty^* L^* \rho_\infty^*}{\mu_\infty^*}, \qquad Pr = \frac{\mu_\infty^* c_p^*}{\kappa_\infty^*}, \qquad \gamma = \frac{c_p^*}{c_v^*} \tag{8}$$

where c_p^* and c_v^* are the gas specific heat coefficients at constant pressure and volume, respectively. The Prandtl transposed boundary conditions at the wall are

$$F = 0, \qquad \frac{\partial Q}{\partial\eta} = 0, \quad \text{and} \quad V = V_w \quad \text{at} \quad \eta = 0 \tag{9a}$$

where

$$V_w = \frac{\sqrt{2\xi Re}}{Q_w U_e \mu_e} v_w \tag{9b}$$

$$Q_w = T_w/T_e \tag{9c}$$

T_w is the adiabatic wall temperature and the physical suction velocity v_w is normalized with respect to U_∞^*. Away from the wall

$$F \to 1 \quad \text{and} \quad Q \to 1 \quad \text{as} \quad \eta \to \infty \tag{10a}$$

To complete the problem formulation, we need to impose initial conditions upstream of the step; that is,

$$F = F(\xi_0,\eta) \quad \text{and} \quad Q = Q(\xi_0,\eta) \quad \text{at} \quad \xi = \xi_0 \tag{10b}$$

and F and Q are taken to correspond to the Blasius flow.

The edge velocity is calculated from the interaction law that relates it to the displacement thickness. Using thin-airfoil theory, we obtain

$$U_e = 1 + \frac{1}{\beta\pi}\int_{LE}^{x} U_e\delta\frac{d(\ell n\,\rho_e)/dt}{x-t}\,dt + \frac{1}{\beta\pi}\int_{LE}^{x}\frac{d\chi/dt}{x-t}\,dt \tag{11}$$

where

$$\beta = \sqrt{1 - M_\infty^2}, \qquad \chi = f + U_e\delta \tag{12a}$$

and the displacement thickness δ is given by

$$\delta = \frac{1}{\sqrt{Re}}\frac{\sqrt{2\xi}}{\rho_e U_e}\int_0^\infty (Q - F)\,d\eta \tag{12b}$$

Integrating Eq. (2), we obtain

$$V_N + K(\eta_N) + V_w = \sqrt{2\xi}\,\frac{\mathrm{d}}{\mathrm{d}\xi}(U_e \xi_e \delta) \tag{13}$$

where

$$K(\eta_N) = \int_0^{\eta_N} \left(Q + 2\xi \frac{\partial Q}{\partial \xi} \right) \mathrm{d}\eta \tag{14}$$

V_N is the vertical velocity at the edge of the boundary layer, and η_N is the corresponding value of η. Following Davis and Werle,[24] Nayfeh et al.,[5] and Al-Maaitah et al.,[21] we integrate Eq. (11) by parts to eliminate the derivative of χ. We assume χ to vary linearly over a differencing interval to obtain a second-order quadratic expression for the edge velocity. By combining the resulting expression with the interaction law, we obtain

$$V_N + \phi \beta_{oi} = \psi - V_w \tag{15}$$

For a definition of ϕ and ψ and a detailed derivation of Eq. (15), we refer the reader to Ref. 5.

Equations (1–3) are solved simultaneously with Eq. (15) using central differencing in the vertical direction and three-point backward differencing in the streamwise direction. The appearance of the suction velocity in the interaction law and the boundary conditions at the wall demands extra care in inverting the resulting matrix. For the flow prescribed, the skin-friction coefficient C_f and the pressure coefficient C_p are defined as

$$C_f = \frac{2U_e^2 \mu(T_w)}{T_w \sqrt{2Re\xi}} \frac{\partial F}{\partial \eta}\bigg|_\eta = 0 \quad \text{and} \quad C_p = 2\frac{\rho_e T_e - 1}{\gamma M_\infty^2}$$

III. Stability Calculations

We consider the linear two-dimensional quasiparallel stability of the mean flow described in Sec. II. Although the quasiparallel assumption has been justified for conventional aerodynamic surfaces, one might question its validity for the configuration under consideration. Because the wavelengths of the disturbances for the geometrical and flow parameters of our configuration are of the same order as those of the Blasius flow at the same Reynolds number and frequency, the nonparallel effects are second-order quantities and to first order the disturbance can be considered to be quasiparallel. Moreover, the direct numerical simulations of Bestek et al.[25] and the experimental results of Dovgal and Kozlov[26] support the quasiparallel assumption. Bestek et al.[25] investigated the influence of a two-dimensional smooth backward-facing step on the spatial development of a Tollmien-Schlichting wave by numerically integrating the Navier-Stokes equations using a finite-difference scheme. The growth rates obtained by the direct numerical simulation are in excellent agreement with those obtained by a quasiparallel theory. Dovgal and Kozlov[26] experimentally investigated the stability characteristics of flows over humps and backward- and forward-facing steps. The experimentally determined transverse and streamwise development of the disturbances ahead, inside, and after the separation bubble is similar to those obtained here and in Refs. 5 and 21 by a quasiparallel theory.

We superimpose on the mean flow two-dimensional disturbances to obtain the total flow quantities:

$$\bar{\rho} = \rho_m(y) + \rho(x,y,t) \tag{16a}$$

$$\bar{u} = u_m(y) + u(x,y,t) \tag{16b}$$

$$\bar{v} = v(x,y,t) \tag{16c}$$

$$\bar{p} = p_m(y) + p(x,y,t) \tag{16d}$$

$$\bar{\mu} = \mu_m(y) + \mu(x,y,t) \tag{16e}$$

$$\bar{\lambda} = \lambda_m(y) + \lambda(x,y,t) \tag{16f}$$

$$\bar{T} = T_m(y) + T(x,y,t) \tag{16g}$$

where the overbar stands for the total-flow quantities while the subscript m stands for the mean-flow quantities. Substituting Eqs. (16) into the compressible Navier-Stokes equations, subtracting the mean-flow quantities, and linearizing the resulting equations, we find that the nondimensional disturbance equations are given by

$$\frac{\partial \rho}{\partial t} + u_m \frac{\partial \rho}{\partial x} + V \mathrm{D}\rho_m + \rho_m \left(\frac{\partial u}{\partial x} + \frac{\partial v}{\partial y} \right) = 0 \tag{17}$$

$$\rho_m \left(\frac{\partial u}{\partial t} + u_m \frac{\partial u}{\partial x} + v \mathrm{D}u_m \right) + \frac{\partial p}{\partial x} - \frac{1}{R}\frac{\partial}{\partial x}\left[r\mu_m \frac{\partial u}{\partial x} + m\mu_m \frac{\partial v}{\partial y} \right] - \frac{1}{R}\frac{\partial}{\partial y}\left[\mu_m \left(\frac{\partial u}{\partial y} + \frac{\partial v}{\partial x} \right) + \mu \mathrm{D}u_m \right] = 0 \tag{18}$$

$$\rho_m \left(\frac{\partial v}{\partial t} + u_m \frac{\partial v}{\partial x} \right) + \frac{\partial p}{\partial y} - \frac{1}{R}\frac{\partial}{\partial y}\left[r\mu_m \frac{\partial v}{\partial y} + m\mu_m \frac{\partial u}{\partial x} \right] - \frac{1}{R}\frac{\partial}{\partial x}\left[\mu_m \left(\frac{\partial v}{\partial x} + \frac{\partial u}{\partial y} \right) + \mu \mathrm{D}u_m \right] = 0 \tag{19}$$

$$\rho_m \left(\frac{\partial T}{\partial t} + u_m \frac{\partial T}{\partial x} + v \mathrm{D}T_m \right) - (\gamma - 1) M_\infty^2 \left(\frac{\partial p}{\partial t} + u_m \frac{\partial p}{\partial x} \right) = \frac{\mu_m}{RPr}\left(\frac{\partial^2 T}{\partial x^2} + \frac{\partial^2 T}{\partial y^2} \right) + \frac{1}{RPr}\frac{\partial \mu}{\partial y}\mathrm{D}T_m + \frac{1}{RPr}\frac{\partial T}{\partial y}\mathrm{D}\mu_m + \frac{(\gamma - 1)M_\infty^2 \phi}{R} + \frac{\mu}{RPr}\mathrm{D}^2 T_m \tag{20}$$

where $\mathrm{D} = \mathrm{d}/\mathrm{d}y$ and

$$\phi = 2\mu_m \left(\frac{\partial u}{\partial y} + \frac{\partial v}{\partial x} \right) \mathrm{D}u_m + \mu (\mathrm{D}u_m)^2 \tag{21}$$

$$m = \lambda_m/\mu_m, \qquad r = 2 + m \tag{22}$$

$$R = \frac{U_\infty^* \delta_0^*}{\nu_\infty^*}, \qquad \delta_0^* = \sqrt{\frac{\nu_\infty^* x^*}{U_\infty^*}} \tag{23}$$

Moreover, for a perfect gas the linearized equation of state can be written as

$$\rho = (\gamma M_\infty^2 p - \rho_m T)/T_m \tag{24}$$

In Eqs. (17–20), the specific heats and the Prandtl number are assumed to be constant. Such an assumption has a small effect on the accuracy of the stability results for the subsonic Mach numbers investigated.

When most of the suction flow is directed normal to the surface and for small suction velocities, Lekoudis[27] showed that the boundary conditions for Eqs. (17–20) can be reasonably expressed as

$$u = v = 0 \qquad \text{at } y = 0 \tag{25}$$

Furthermore, for high-frequency disturbances, we have

$$T = 0 \qquad \text{at } y = 0 \tag{26}$$

while far away from the wall

$$u, v, p, T \to 0 \qquad \text{as } y \to \infty \tag{27}$$

Assuming that $\bar{\gamma}$ and $\bar{\mu}$ are functions of temperature only, we define λ and μ as

$$\lambda = \frac{d\lambda_m}{dT_m} T = \lambda'_m(T_m)T \qquad \text{and} \qquad \mu = \frac{d\mu_m}{dT_m} T = \mu'_m(T_m)T \tag{28}$$

Because the coefficients in Eqs. (17–21) are functions of y only, we can expand u,v,p, and T in the form of traveling harmonic waves as

$$u = \hat{u}(y) \exp\left[i \int \alpha \, dx - i\omega t \right] \tag{29a}$$

$$p = \hat{p}(y) \exp\left[i \int \alpha \, dx - i\omega t \right] \tag{29b}$$

$$v = \hat{v}(y) \exp\left[i \int \alpha \, dx - i\omega y \right] \tag{29c}$$

$$T = \hat{T}(y) \exp\left[i \int \alpha \, dx - i\omega t \right] \tag{29d}$$

where α and ω are the wavenumber and frequency, respectively. Substituting Eqs. (28) and (29) into Eqs. (17–20), dropping the caret for convenience, and defining

$$\Omega = \omega - \alpha u_m \tag{30}$$

we obtain

$$\mathrm{D}v = -i\alpha u + \frac{\mathrm{D}T_m}{T_m} v + \frac{i\Omega p}{p_m} - \frac{i\Omega T}{T_m} \tag{31}$$

$$\mathrm{D}^2 u = \left(\frac{-i\rho_m \Omega R}{\mu_m} + r\alpha^2 \right) u - \frac{\mu'_m \mathrm{D}T_m}{\mu_m} \mathrm{D}u + \left[\frac{\rho_m R \, \mathrm{D}u_m}{\mu_m} - i\alpha \frac{\mu'_m \, \mathrm{D}T_m}{\mu_m} \right] v - i(1+m)\alpha \, \mathrm{D}v + \frac{iR\alpha}{\mu_m} p - \left[\frac{\mathrm{D}u_m}{\mu_m} \mathrm{D}(\mu'_m) + \frac{\mathrm{D}^2 u_m}{\mu_m} \mu'_m \right] T - \frac{\mu'_m}{\mu_m} \mathrm{D}u_m \mathrm{D}T \tag{32}$$

$$\chi_0 \, \mathrm{D}p = -i\alpha \left(r \frac{\mathrm{D}T_m}{T_m} + \frac{2\mu'_m \, \mathrm{D}T_m}{\mu_m} \right) u - i\alpha \, \mathrm{D}u + \left(\frac{iR\Omega}{\mu_m T_m} - \alpha^2 + r \frac{\mathrm{D}^2 T_m}{T_m} + \frac{r\mu'_m (\mathrm{D}T_m)^2}{\mu_m T_m} \right) v + i \frac{r}{p_m} \left[\Omega \left(\frac{\mathrm{D}T_m}{T_m} + \frac{\mu'_m}{\mu_m} \mathrm{D}T_m \right) - \alpha \mathrm{D}u_m \right] p + \left[i(\alpha \mathrm{D}u_m) \left(\frac{\mu'_m}{\mu_m} + \frac{r}{T_m} \right) - \frac{ir\Omega\mu_m}{\mu_m} \mathrm{D}T_m \right] T - \frac{ir\Omega}{T_m} \mathrm{D}T \tag{33}$$

$$\mathrm{D}^2 T = -2(\gamma - 1) M_\infty^2 \, Pr \, \mathrm{D}u_m \mathrm{D}u + \left[RPr \frac{\rho_m \mathrm{D}T_m}{\mu_m} - 2i(\gamma - 1) M_\infty^2 \, Pr \alpha \mathrm{D}u_m \right] v + i(\gamma - 1) M_\infty^2 \, PrR \frac{\Omega}{\mu_m} p + \left[-iRPr\Omega \frac{\rho_m}{\mu_m} + \alpha^2 - \frac{(\mathrm{D}T_m)^2 \mu'_m}{\mu_m} - \mu'_m \frac{\mathrm{D}^2 T_m}{\mu_m} - (\gamma - 1) M_\infty^2 \, Pr \frac{\mu'_m}{\mu_m} (\mathrm{D}u_m)^2 \right] T - 2 \frac{\mu'_m \mathrm{D}T_m}{\mu_m} \mathrm{D}T \tag{34}$$

$$u = v = T = 0 \qquad \text{at } y = 0 \tag{35}$$

$$u,v,p,T, \to 0 \quad \text{as} \quad y \to \infty \tag{36}$$

where

$$\chi_0 = \frac{R}{\mu_m} - ir \frac{\Omega}{p_m}, \qquad p_m = \frac{1}{\gamma M_\infty^2} \tag{37}$$

The system of Eqs. (31–36) represents an eigenvalue problem for the parameters α, ω and R. For known mean-flow velocity profiles, the eigenvalue and corresponding eigenfunction are calculated using the finite-difference subroutine DBVPFD.[28] The results of DBVPFD are in full agreement with those of SUPORT,[29] but the finite-difference code is much faster. Specifying R and ω to be real, we find the eigenvalue

$$\alpha = \alpha_r + i\alpha_i \tag{38}$$

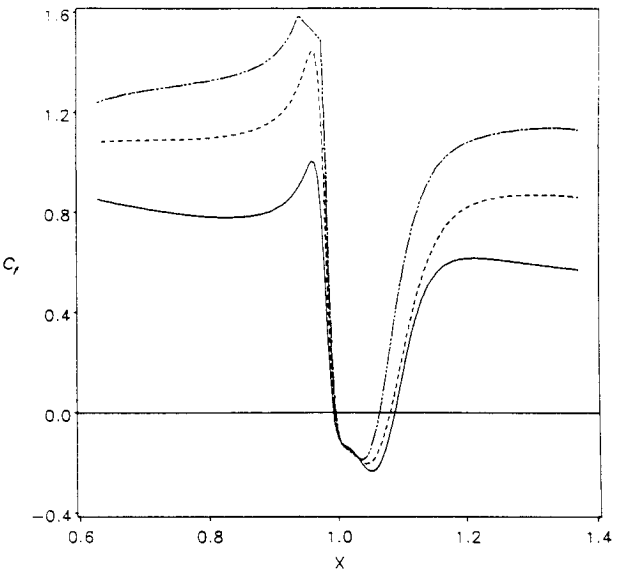

Fig. 2 Effect of wall suction on the shear coefficient for a flow over a backward-facing step when the step height = 0.003, step slope = −4.35, $M_\infty = 0.8$, $Re = 1.0 \times 10^6$, and $Pr = 0.72$. —— $v_w = 0.0$, – – – $v_w = 3.0 \times 10^{-4}$, and — · · — $v_w = 5.0 \times 10^{-4}$.

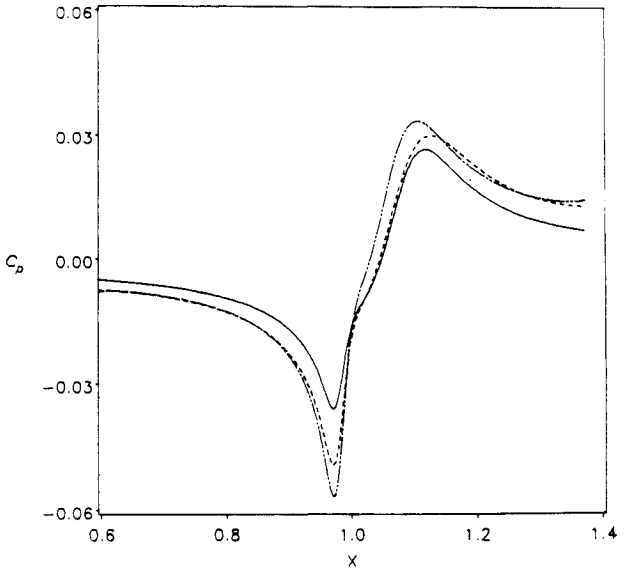

Fig. 3 Effect of wall suction on the pressure coefficients for a flow over a backward-facing step when the step height = 0.003, step slope = −4.35, $M_\infty = 0.8$, $Re = 1.0 \times 10^6$, and $Pr = 0.72$. —— $v_w = 0.0$, – – – $v_w = 3.0 \times 10^{-4}$, and — · · — $v_w = 5.0 \times 10^{-4}$.

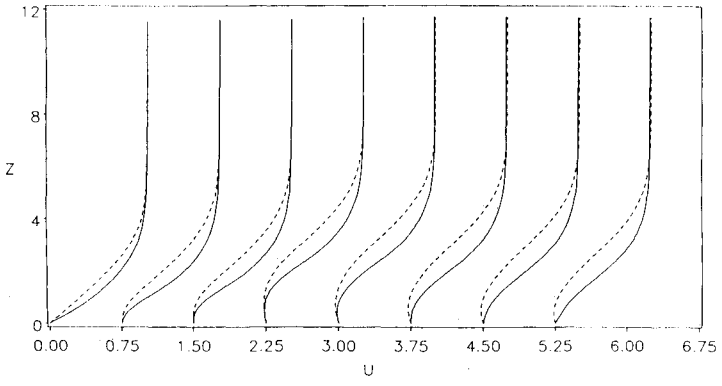

Fig. 4 Effect of wall suction on the streamwise velocity profiles along the plate when the step height = 0.003, step slope = −4.35, $M_\infty = 0.8$, $Re = 1.0 \times 10^6$, and $Pr = 0.72$. The profiles correspond to the following values of R starting from left to right: 897, 1000, 1010, 1020, 1030, 1034, and 1042. - - - $v_w = 0.0$ and — — $v_w = 5.0 \times 10^{-4}$.

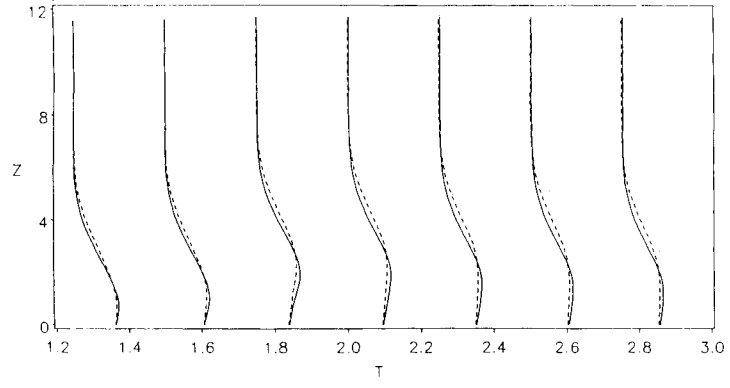

Fig. 5 Effect of wall suction on the temperature profiles along the plate when the step height = 0.003, step slope = −4.35, $M_\infty = 0.8$, $Re = 1.0 \times 10^6$, and $Pr = 0.72$. The profiles correspond to the following vaues of R starting from left to right: 897, 1000, 1010, 1020, 1030, 1034, and 1042. - - - $v_w = 0.0$ and — — $v_w = 5.0 \times 10^{-4}$.

where α_r and α_i are the real and imaginary parts of α, respectively. Then $-\alpha_i$ is the spatial growth rate of the disturbance.

The amplification factor is calculated from α_i as

$$N = -2 \int_{R_0}^{R} \alpha_i(R)\, dR \tag{39}$$

where R_0 corresponds to the position where the constant-frequency disturbance first becomes unstable. For the flows investigated, the growth rates can have a negative value at more than one location. In such cases, the amplification factor is set to be zero whenever it turns out to be negative. We calculate it using Eq. (39) when the disturbance starts to grow again.

IV. Results and Discussion

First, we investigate the influence of suction on the mean-flow characteristics. Figure 2 shows the effect of continuous suction on the skin-friction coefficient of flows over a backward-facing step located at $x = 1.0$. As expected, suction reduces the size of the separation bubble. Hahn and Pfenninger[15] reported a reduction of 20% in the separation region. When $v_w = 5 \times 10^{-4}$ the size of the separation bubble reduces to 67% of that when no suction is applied. Moreover, suction increases the positive shear in the attached flow region and decreases the negative shear in the separated flow region. Figure 3 shows the effect of continuous suction on the pressure coefficient C_p. Although continuous suction does not have much effect on C_p far away from the step, it results in steeper pressure gradients around it. At different locations on the plate, Fig. 4 shows a comparison between the mean profiles when $v_w = 0.0$ and $v_w = 5 \times 10^{-4}$. Away from separation, suction results in fuller velocity profiles. This is also true in the separation region; however, the generalized inflection point moves closer to the wall. For the same conditions, Fig. 5 shows that suction slightly alters the temperature profiles. Outside the separation bubble, Fig. 6 shows that suction reduces the vorticity throughout the boundary layer except near the wall. However, in the separation region, suction

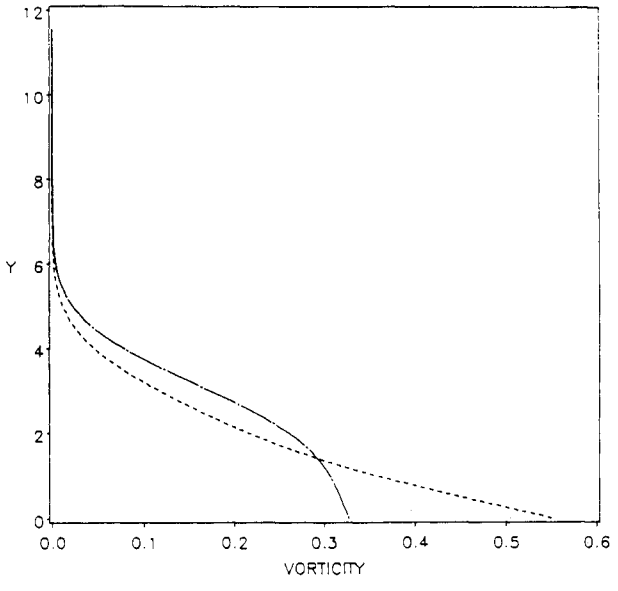

Fig. 6 Influence of suction on the first derivative of the velocity profile at $x = 0.8$ when the step height = 0.003, step slope = −4.35, $M_\infty = 0.8$, $Re = 1.0 \times 10^6$, and $Pr = 0.72$. —·— $v_w = 0.0$ and - - - $v_w = 5.0 \times 10^{-4}$.

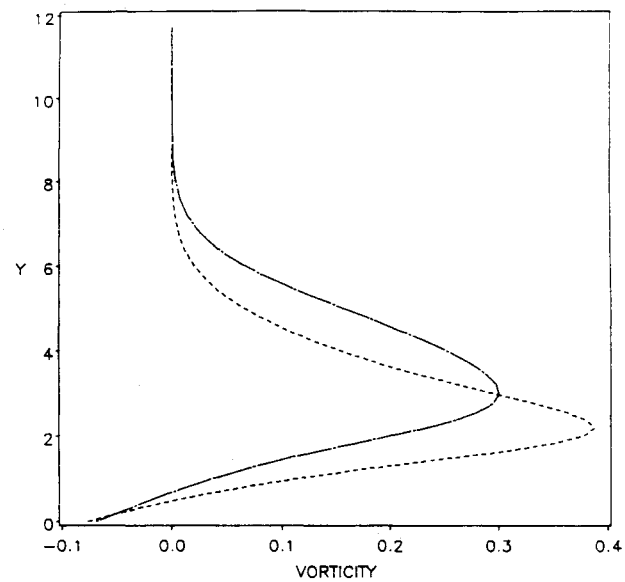

Fig. 7 Influence of suction on the first derivative of the velocity profile at $x = 1.04$ when the step height $= 0.003$, step slope $= -4.35$, $M_\infty = 0.8$, $Re = 1.0 \times 10^6$, and $Pr = 0.72$. — · — $v_w = 0.0$ and - - - $v_w = 5.0 \times 10^{-4}$.

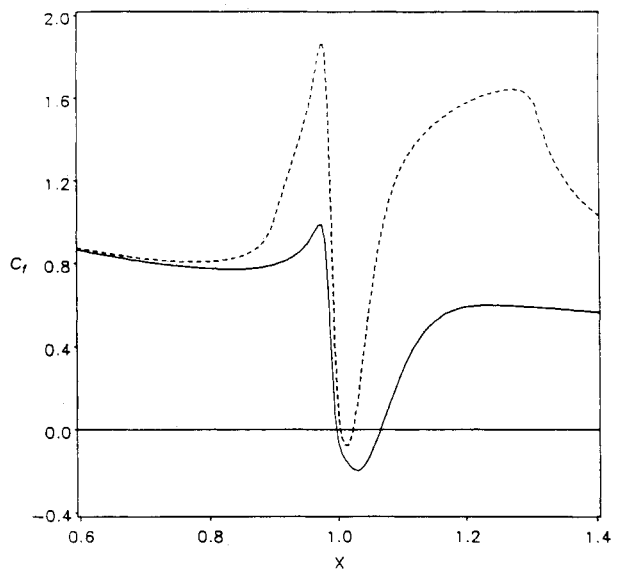

Fig. 9 Effect of a concentrated suction strip on the shear coefficient. The strip starts at $x = 0.9$ and ends at $x = 1.3$, $v_w = 1.0 \times 10^{-3}$, step height $= 0.002$, step slope $= -4.35$, $M_\infty = 0.8$, $Re = 10 \times 10^6$, and $Pr = 0.72$. —— without suction and - - - with suction.

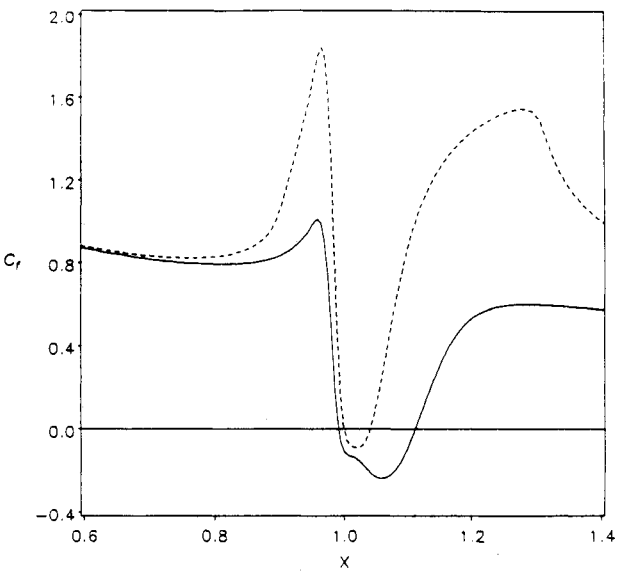

Fig. 8 Effect of a concentrated suction strip on the shear coefficient. The strip starts at $x = 0.9$ and ends at $x = 1.3$, $v_w = 1.0 \times 10^{-3}$, step height $= 0.003$, step slope $= -4.35$, $M_\infty = 0.8$, $Re = 1.0 \times 10^6$, and $Pr = 0.72$. —— without suction and - - - with suction.

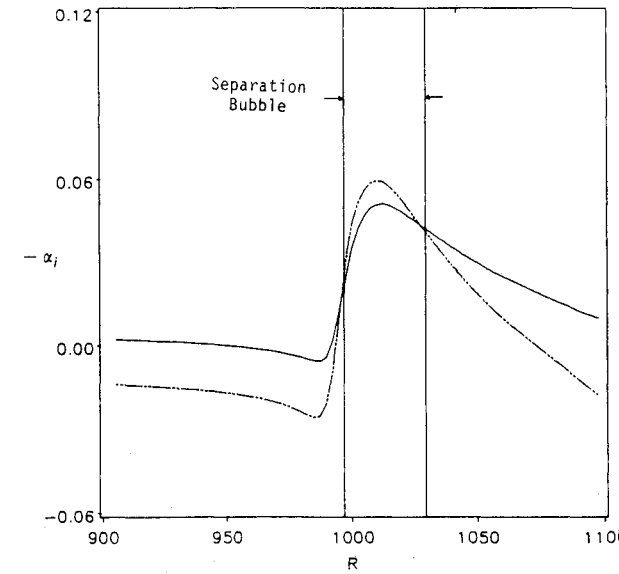

Fig. 10 The growth rates for the flow over steps with and without continuous suction when the step height $= 0.003$, step slope $= -4.35$, $M_\infty = 0.8$, $Re = 1.0 \times 10^6$, $Pr = 0.72$, and $F = 50 \times 10^{-6}$. —— $v_w = 0.0$ and — ·· — $v_w = 5.0 \times 10^{-4}$.

widens the region of increase in the vorticity, as shown in Fig. 7.

Figure 8 shows that the size of the separation bubble is reduced significantly when a concentrated suction strip is placed around the step. The strip starts at $x = 0.9$ and ends at $x = 1.3$, $v_w = 1 \times 10^{-3}$, $M_\infty = 0.8$, and the height of the step is $0.003L^*$. The resulting separation bubble extends over a distance of $0.04L^*$, which is 22% of the size when no suction is applied. For the same conditions but with the step height $= 0.002L^*$, Fig. 9 shows that the separation bubble extends over a distance of $0.017L^*$, which is 25% of that when no suction is applied. Figures 8 and 9 show a large increase in the positive shear around the suction strips.

Next, we analyze the stability characteristics of the mean profiles calculated using the IBL equations. Figure 10 shows the growth rates for the case when $v_w = 5 \times 10^{-4}$ and $v_w = 0.0$. Outside the separation region, suction stabilizes the boundary layer due to the resulting fuller velocity profiles. In the separation bubble, suction has a destabilizing influence on the boundary layer due to the movement of the inflection point toward the wall and the increase in the vorticity near the wall. Figure 11 shows the growth rates for different suction levels. As v_w increases, the flow is stabilized in the attached flow region and destabilized in the separation region. A similar trend was noted in the case of wall cooling. Whereas the variation of the N factor with wall temperature has a relative minimum, Fig. 12 shows that the N factor monotonically decreases with suction. Thus, increasing the suction level results in a greater reduction in the overall N factor and hence in stabilizing the boundary layer. This is due to the significant reduction in the separation bubble.

To optimize the effect of the suction strips, Reed and

Nayfeh[12] suggested that they be placed around the smallest-growth-rate location. In the flow over backward-facing steps, these regions are near branch I of the neutral-stability curve of the Blasius flow, slightly ahead of the step, and around the end of separation. To study the effect of suction-strip distributions, we locate three suction strips of width $0.2L^*$ at $x = 0.360$, 0.723, and 1.103, each having a $v_w = 2.33 \times 10^{-4}$. The total flow rate equals that when continuous suction is applied with $v_w = 1.0 \times 10^{-4}$ from the leading edge to a distance of $1.4L^*$. In Fig. 13, we compare the growth rates obtained using the suction strips with those obtained using a continuous-suction distribution with $v_w = 1.0 \times 10^{-4}$ and the case of no suction. In the case of suction strips, the growth rates are lower than those corresponding to $v_w = 0.0$ except in the separation bubble. However, they are lower than those corresponding to the continuous suction case only around the strip locations, with the exception of the separation region. The strips gradually decrease the growth rate near the beginning of the strips. Their effect, however, continues downstream of the strips. A similar trend was noted by Reed and Nayfeh[12] and Hahn and Pfenninger.[15] The resulting N factors shown in Fig. 14 demonstrate that the same amount of flow rate can stabilize the flow more when properly distributed in strips. Although in Ref. 15 suction was placed only downstream of the step, suction was found to be most effective when placed near the reattachment region. This corresponds to the place where the third strip is located in the present work.

As discussed previously in Figs. 8 and 9, the separation bubble can be reduced significantly when a concentrated suction strip is placed across it. Figures 15 and 16 show the resulting N factors for the same flow conditions of Figs. 8 and 9, respectively. The maximum N factor in Fig. 15 was reduced from 9.0 to 4.0. In Fig. 16, the effect of separation was nearly eliminated.

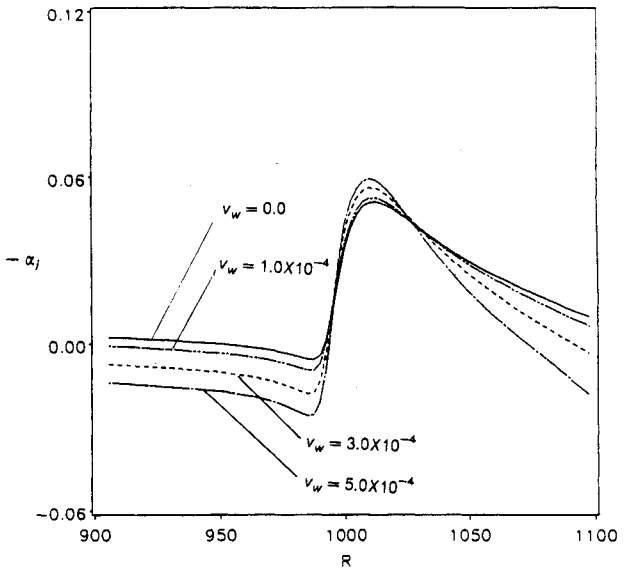

Fig. 11 The variation of the growth rates with streamwise location for different continuous suction levels: step height = 0.003, step slope = −4.35, $M_\infty = 0.8$, $Re = 1.0 \times 10^6$, $Pr = 0.72$, and $F = 50 \times 10^{-6}$.

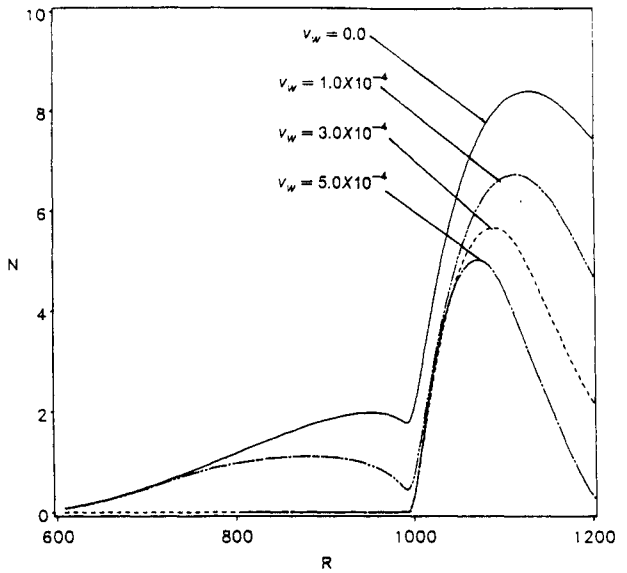

Fig. 12 The variation of the amplification factor with streamwise location for different continuous suction levels: step height = 0.003, step slope = −4.35, $M_\infty = 0.8$, $Re = 1.0 \times 10^6$, $Pr = 0.72$, and $F = 50 \times 10^{-6}$.

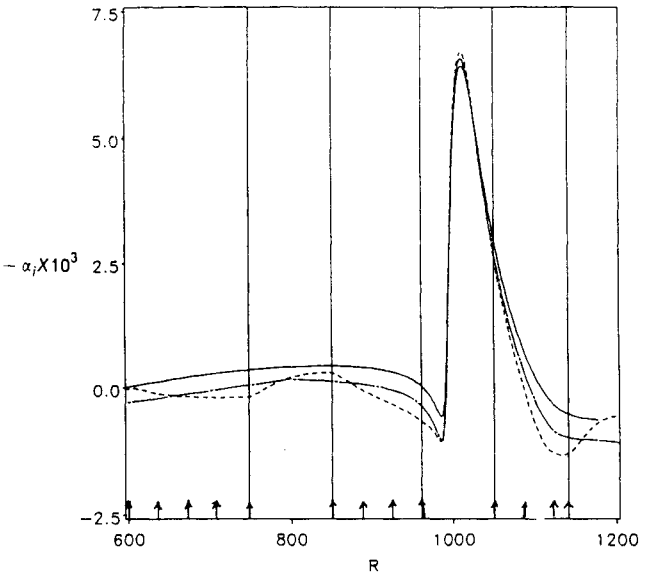

Fig. 13 The effect of suction strips and continuous suction on the growth rates for the flow over a step with a height of 0.003, step slope = −4.35, $M_\infty = 0.5$, $Re = 1.0 \times 10^6$, $Pr = 0.72$, and $F = 50 \times 10^{-6}$. The suction strips are centered at $R = 678$, 907, and 1097 with a length of $0.2L^*$ each. In the case of strips $v_w = 2.33 \times 10^{-4}$, and in the case of continuous suction $v_w = 1.0 \times 10^{-4}$. —— no suction, — · — continuous suction, and – – – suction strips.

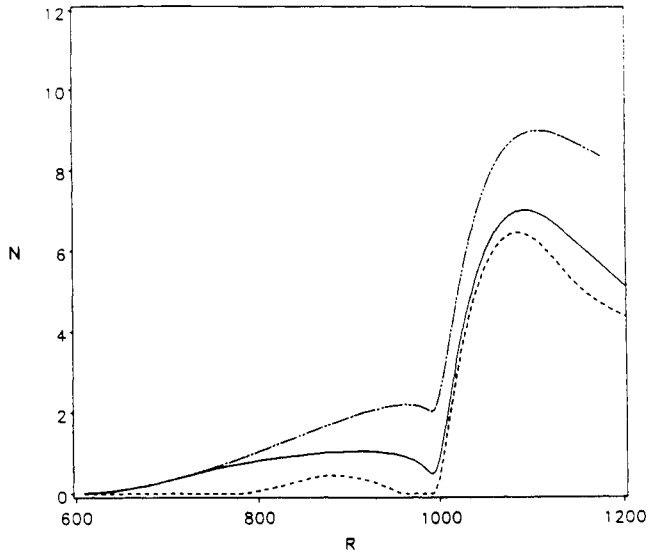

Fig. 14 Comparison of the variation of the amplification factor with streamwise location for the cases of continuous suction, suction strips, and no suction. Flow conditions are the same as in Fig. 13. — ·· — no suction, —— continuous suction, and – – – suction strips.

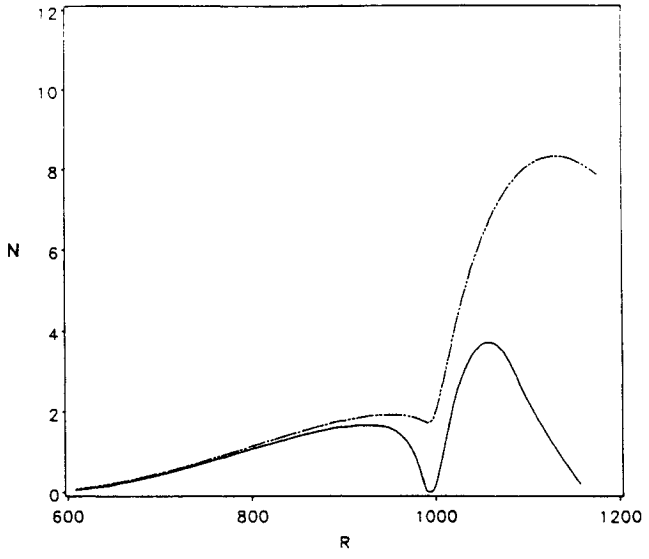

Fig. 15 Effect of the concentrated strip suction described in Fig. 8 on the amplification factor. Flow conditions are the same as in Fig. 8, $F = 50 \times 10^{-6}$. — ·· — no suction and —— suction strip.

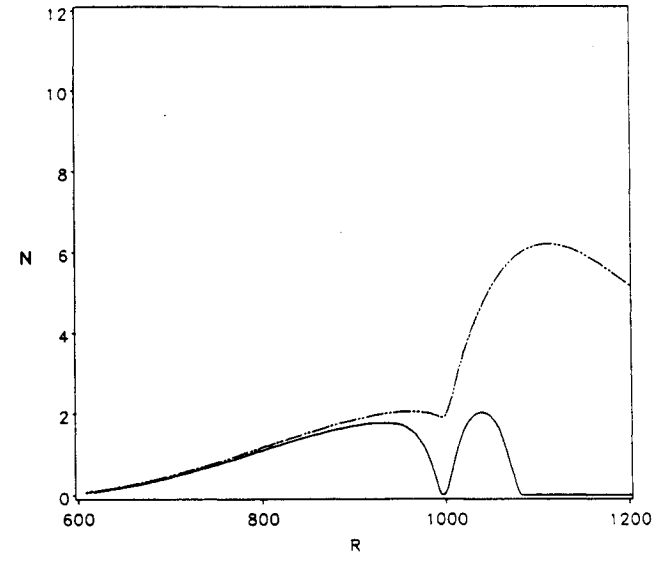

Fig. 16 Effect of the concentrated strip suction described in Fig. 9 on the amplification factor. Flow conditions are the same as in Fig. 9, $F = 50 \times 10^{-6}$. — ·· — no suction and —— suction strip.

The stability characteristics are calculated for the most dangerous frequency.[5,20] Suction does not have much effect on this frequency. Figure 17 shows the N factors for different frequencies when continuous suction is applied. The trend is similar in the case of suction strips.

In conclusion, we note that suction reduces the viscous instability and increases the shear-layer instability. Although cooling loses its efficiency as the wall temperature decreases below a critical value, increasing the suction results in a monotonic stabilization of the boundary layer owing to the significant reduction in the separation bubble by suction. Properly distributing suction in strips results in more stabilization of the boundary layer. Moreover, concentrating the suction in the separation region can eliminate the effect of the separation bubble.

Acknowledgment

This work was supported by the Office of Naval Research under Grant N00014-85-K-0011 and the National Aeronautics and Space Administration under Grant NAG-1-714.

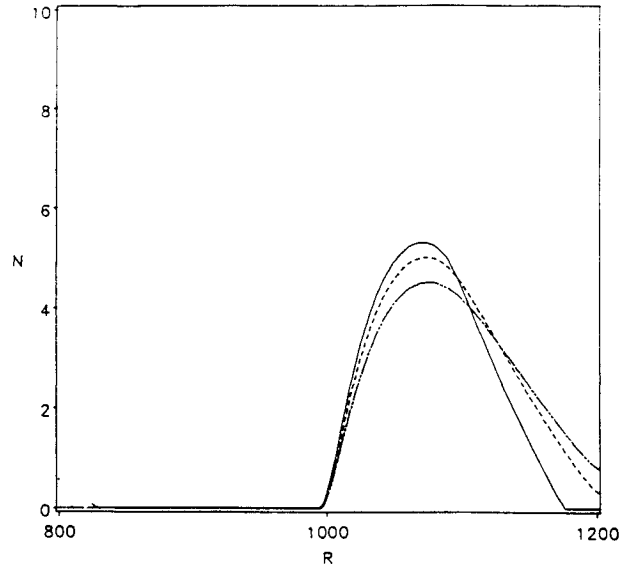

Fig. 17 The variation of the amplification factor with streamwise location for flows over steps with continuous wall suction for different frequencies when the step height = 0.003, step slope = −4.35, $M_\infty = 0.5$, $Re = 1.0 \times 10^6$, $v_w = 5 \times 10^{-4}$, and $Pr = 0.72$. — ·· — $F = 40 \times 10^{-6}$, —— $F = 50 \times 10^{-6}$, and - - - $F = 60 \times 10^{-6}$.

References

[1]Van Dam, C. P., and Holmes, B. J., "Boundary-Layer Transition Effects on Airplane Stability and Control," *Journal of Aircraft*, Vol. 25, Aug. 1988, pp. 702–709.

[2]Holmes, B. J., Obara, C. J., Martin, G. L., and Domack, C. S., "Manufacturing Tolerances for Natural Laminar Flow Air Frame Surfaces," NASA CP-2413, 1986.

[3]Holmes, B. J., Obara, C. J., and Yip, L. P., "Natural Laminar Flow Flight Experiments on Modern Airplane Surfaces," NASA TP-2256, June 1984.

[4]Goldstein, M. E., "Scattering of Acoustic Waves into Tollmien-Schlichting Waves by Small Streamwise Variation in Surface Geometry," *Journal of Fluid Mechanics*, Vol. 154, 1985, pp. 509–528.

[5]Nayfeh, A. H., Ragab, S. A., and Al-Maaitah, A. A., "Effect of Bulges on the Stability of Boundary Layers," *Physics of Fluids*, Vol. 31, April 1988, pp. 796–806.

[6]Carmichael, B. H., Whites, R. C., and Pfenninger, W., "Low-Drag Boundary-Layer Suction Experiment in Flight on the Wing Glove of a F-94A Airplane," Northrup Aircraft Rept. NAI-57-1163 (BLC-101), 1957.

[7]Carmichael, B. H., and Pfenninger, W., "Surface Imperfection Experiments on a Swept Laminar Suction Wing," Northrup Aircraft Rept. NOR-59-454 (BLC-124), 1959.

[8]Carmichael, B. H., "Surface Waviness Criteria for Swept and Unswept Laminar Suction Wings," Northrup Aircraft Rept. NOR-59-438 (BLC-123), 1957.

[9]Spence, O. A., and Randall, D. G., "The Influence of Surface Waves on the Stability of a Laminar Boundary Layer with Uniform Suction," British Aeronautical Research Council Rept. 2241, 1954.

[10]Lin, C. C., "On the Stability of Two-Dimensional Parallel Flows," *Quarterly of Applied Mathematics*, Vol. 3, 1945, pp. 117–142, 218–234, 277–301.

[11]Nayfeh, A. H., and Reed, H. L., "Stability of Flows Over Axisymmetric Bodies with Porous Suction Strips," *Physics of Fluids*, Vol. 28, Oct. 1985, pp. 2990 2998.

[12]Reed, H. L., and Nayfeh, A. H., "Numerical Perturbation Techniques for Stability of Flat-Plate Boundary Layers with Suction," *AIAA Journal*, Vol. 24, Feb. 1986, pp. 208–214.

[13]Reynolds, G. A., and Saric, W. S., "Experiments on the Stability of Flat-Plate Boundary Layers with Suction," *AIAA Journal*, Vol. 24, Feb. 1986, pp. 202 207.

[14]Saric, W. S., and Reed, H. L., "Effect of Suction and Weak Mass Injection on Boundary-Layer Transition," *AIAA Journal*, Vol. 24, March 1986, pp. 383 389.

[15]Hahn, M., and Pfenninger, W., "Prevention of Transition Over a Backward Step by Suction," *Journal of Aircraft*, Vol. 20, 1973, pp. 618 622.

[16]Srokowski, A. J., and Orszag, S. A., "Mass Flow Requirements for LFC Wing Design," AIAA Paper 77-1222, Aug. 1977.

[17]Hefner, J. N., and Bushnell, D. M., "Application of Stability Theory to Laminar Flow Control," AIAA Paper 79-1493, July 1979.

[18]Fage, A., "The Smallest Size of Spanwise Surface Corrugation which Affect Boundary-Layer Transition on an Airfoil," British Aeronautical Research Council Rept. 2120, Jan. 1943.

[19]Cebeci, T., and Egan, D. A., "Effect of Wave-Like Roughness on Transition," AIAA Paper 88-0139, Jan. 1988.

[20]Ragab, S. A., Nayfeh, A. H., and Krishna, R. C., "Stability of Compressible Boundary Layers over a Smooth Backward Facing Step," AIAA Paper 90-1449, June 1990.

[21]Al-Maaitah, A. A., Nayfeh, A. H., and Ragab, S. A., "Effect of Wall Cooling on the Stability of Compressible Subsonic Flows Over Smooth Two-Dimensional Backward-Facing Steps," *Physics of Fluids*, Vol. A2, March 1990, pp. 381-389.

[22]Davis, R. T., "A Procedure for Solving the Compressible Interacting Boundary-Layer Equations for Subsonic and Supersonic Flows," AIAA Paper 87-1414, June 1987.

[23]Chang, K. C., Alemdaroglu, N., Mehfa, U., and Cebeci, T., "Further Comparison of Interactive Boundary-Layer and Thin-Layer Navier-Stokes Procedures," *Journal of Aircraft*, Vol. 25, Oct. 1988, pp. 897-903.

[24]Davis, R. T., and Werle, M. J., "Progress on Interacting Boundary-Layer Computations at High Reynolds Number," *Numerical and Physical Aspect of Aerodynamic Flows*, edited by T. Cebeci, Springer, Berlin, 1982, pp. 187-192.

[25]Bestek, H., Gruber, K., and Fasel, H., "Numerical Investigation of Unsteady Laminar Boundary-Layer Flows Over Backward-Facing Steps," The Fourth Asian Congress of Fluid Mechanics, Hong Kong, Aug. 1989.

[26]Dovgal, A. V., and Kozlov, V. V., "Hydrodynamic Instability and Receptivity of Small-Scale Separation Regions," The Third IUTAM Symposium on Laminar-Turbulent Transition, Toulouse, France, Sept. 1989.

[27]Ledoudis, S. G., "Stability of Boundary Layers Over Permeable Surfaces," AIAA Paper 87-203, Jan. 1987.

[28]Pereyra, V., "PASAV3: An Adaptive Finite-Difference Fortran Program for First-Order Nonlinear Ordinary Boundary-Value Problems," *Lecture Notes in Computer Science*, Vol. 76, edited by B. Childs, M. Scott, J. W. Daniel, E. Denman, and P. Nelson, Springer, Berlin, 1976, pp. 67-88.

[29]Scott, M. R., and Watts, H. A., "Computational Solution of Linear Two-Point Boundary-Value Problems Via Orthonormalization," *SIAM Journal on Numerical Analysis*, Vol. 14, March 1977, pp. 40-70.